Artificial intelligence for the removal of benzene, toluene, ethyl benzene and xylene (BTEX) from aqueous solutions using iron nanoparticles

Ahmed S. Mahmoud, Mohamed K. Mostafa and Soha A. Abdel-Gawad

ABSTRACT

Magnetic nanosorbents proved to be highly effective in inorganic and organic contaminants removal from aqueous solutions, especially nano zero valent iron (nZVI). The main purpose of this study is to investigate the effect of using nZVI in removing benzene, toluene, ethyl benzene and xylene (BTEX) contaminants from aqueous solutions. The nZVI and the standard BTEX solution were prepared in the laboratory. X-ray diffraction (XRD), UV spectrophotometry, and scanning electron microscopy (SEM) analysis were used for nZVI characterization. The effects of contact time, initial BTEX mixture concentration, adsorbent dose, temperature, and pH on the amount of BTEX absorbed were investigated. The highest removal efficiency of 97% for the BTEX mixture was achieved at a stirring rate of 100 rpm, temperature of 60°C, and pH 7. The minimum effective time for efficient removal was 30 min, while the effective dose for BTEX compounds removal was 0.22 g/L. The Freundlich model was the best fit of experimental data. An artificial neural network (ANN) was used to predict the BTEX removal efficiency. Modeling results showed that ANN with average absolute error of 0.6272% is reliable in describing the adsorption of BTEX onto the iron nanoparticles. It is estimated that the cost of BTEX removal by nZVI under the optimal conditions will be about 3.5 USD per cubic meter.

Key words | adsorption, artificial neural network, BTEX removal, degradation, iron nanoparticles

Ahmed S. Mahmoud (corresponding author)
Sanitary and Environmental Institute (SEI),
Housing and Building National Research Center (HBRC),
87 Tahrir Street, Dokki, Giza, P.O. Box 1770,
Egypt
E-mail: *ahmeds197@gmail.com*

Mohamed K. Mostafa
Environmental Engineering Program,
Zewail City of Science and Technology,
6th of October City, Giza Governorate 12588,
Egypt

Soha A. Abdel-Gawad
Chemistry Department,
Faculty of Science, Cairo University, Giza,
Egypt

INTRODUCTION

Volatile organic compounds (VOCs) are solid or liquid organic compounds that can easily evaporate into a gaseous state (Gorelick & Gvirtzman 1995). VOCs are contaminants of concern in surface water because special techniques are required for them to be removed from water, and in groundwater due to their tendency to migrate to drinking water wells. In 1997, the Agency of Toxic Substances and Disease Registry (ATSDR) determined that VOCs are considered a public health hazard (Crosse *et al.* 2007). There are different sources of surface and ground water contamination by VOCs such as urban runoff, industrial activity, leaking of underground storage tanks, landfills, and improper disposal of solvents, petroleum products, dyes, and paints (Edil 2003; Zhang *et al.* 2004). The use of chlorinated solvents, the most common VOCs found in drinking water, was common for a long time in many industries (Lee *et al.* 2002; Moran *et al.* 2007). Increasing concentrations of VOCs in drinking water may cause damage to the liver, kidney, nervous, and immune systems (Kampa & Castanas 2008; Pronczuk & Surdu 2008). BTEX, which includes benzene, toluene, ethyl benzene and xylene, is a group of VOCs (Davidson & Creek 2000; Stern & Lagos 2008). BTEX compounds are often found in coal tar, crude petroleum, and petroleum products. BTEX compounds are classified as a human carcinogen and genotoxic substances (Stern & Lagos 2008; Mazzeo *et al.* 2011). BTEX typically form about 18% by

doi: 10.2166/ws.2017.225

weight of a typical gasoline blend (Falta *et al.* 2005). BTEX compounds recently have received much attention because they constitute a serious threat to groundwater reservoirs. Different techniques are used for in-situ remediation of the BTEX compounds, such as air stripping systems, chemical oxidation, and thermal treatment (LaGrega *et al.* 2001). These techniques are not widely used in BTEX remediation due to the high cost of operation. Recently, adsorption has become more common in treating water laden with BTEX compounds.

Magnetic nanosorbents, such as nano zero valent iron (nZVI), have been proven to be effective in transforming and detoxifying a wide variety of contaminants, such as polychlorinated biphenyls (PCBs), chlorinated organic solvents, and pesticides (Rahman *et al.* 2014). The adsorption process involves: (1) transport of the BTEX compounds from the solution to the nZVI surface; (2) adsorption on the surface of nZVI particles; and (3) transport within the nZVI (Rahman *et al.* 2014). NZVI could provide a cost-effective solution to the BTEX remediation problem because applying this technology does not require specific equipment (Zhao *et al.* 2008). NZVI particles are extremely small with a diameter normally ranging from 20 to 60 nm leading to an increased surface area to volume ratio and thus increased reactivity (Rahman *et al.* 2014). Because of its high surface area which allows a greater possibility of coming into contact with BTEX compounds, nZVI is thought to offer a better alternative to the traditional methods of treating water laden with BTEX compounds (Rahman *et al.* 2014). Other advantages of applying this technology are the availability of raw materials, the low-cost production process of nZVI, and the ease of iron nanoparticles separation from the solution after treatment using magnetic power (Stefaniuk *et al.* 2016). The iron nanoparticles are also characterized by high stability due to the excess amounts of sodium borohydride and ethanol used during the preparation process, which reduce the possibility of iron nanoparticles oxidizing to iron oxide (Giasuddin *et al.* 2007). The main drawbacks of using this technology are: (1) the high reactivity of nZVI which should be used alone without any surfactants, (2) the increase in the pH of the treated water which can be undesirable, (3) the nZVI can easily be dissolved in the presence of hydrochloric acid (HCl), so the use of sulfuric acid (H_2SO_4) and phosphoric acid (H_3PO_4) is preferred for acidification, and (4) the solubility of some nZVI in the solution, especially in acidic media (Gautam & Chattopadhyaya 2017).

Several studies have been conducted to study the effect of using nZVI in the removal of organic compounds. Raychoudhury & Scheytt (2013) conducted research to study the effect of using nZVI in the removal of organic compounds that were mostly composed of xenobiotics (Raychoudhury & Scheytt 2013). The results of their study showed that azo compounds, as well as nitro organic compounds, including pesticides, commercial compounds, explosives, and pharmaceuticals are highly interactive with nZVI. The chlorinated hydrocarbons (i.e., carbon tetrachloride, TCE) showed higher reaction rates with nZVI when compared to chlorinated compounds with complex structures or higher molecular weights (PCBs, ICM, PBDEs, DDT) (Raychoudhury & Scheytt 2013). Abdel-Gawad *et al.* (2016) conducted research to study the effect of using nZVI in the removal of polyaromatic hydrocarbons (PAHs) that are considered to be the most dangerous organic contaminants. The results of their study showed that the nZVI was effective in removing PAHs from aqueous solutions. The maximum removal efficiency was 56% at a stirring rate of 100 rpm, pH 7, 30 min contact time, 0.2 g/L of nZVI, and PAH concentration of 37 μg/L.

The main purpose of this study is to investigate the best conditions for BTEX compounds removal from aqueous solutions using nZVI and to find the relationships between the BTEX compounds removal efficiency and the change in contact time, initial BTEX mixture concentration, adsorbent dose, stirring rate, pH, and temperature. Freundlich and Langmuir isotherm models were performed in order to accurately describe the equilibrium sorption data. The artificial neural network (ANN) technique was also used to find the correlation between the studied parameters and the BTEX removal efficiency.

METHODS

Chemicals and reagents

The following chemicals were used in this study. Iron chloride hexahydrate ($FeCl_3.6H_2O$, 98.5% pure) was obtained

from Arabic Laboratory Equipment Company. Sodium hydroxide (NaOH, 99% pure) was purchased from Oxford Company. Sodium borohydride ($NaBH_4$, 99% pure) was obtained from Win Lab Company. Calcium chloride ($CaCl_2$, ACS grade) was obtained from BDH Chemicals. Sulfuric acid (H_2SO_4, 95–97%) was purchased from Honeywell Company. BTEX mix was purchased from Supelco Company (6 BTEX compound 2,000 µg pure, methanol). Potassium chromate ($KCrO_4$, 99.5% pure) was obtained from Kano Chemical Company. Dichloromethane (CH_2Cl_2, HPLC grade) was obtained from Fisher Scientific UK Company. Ethanol (C_2H_6O, 95% pure) was purchased from World Company supplying submarine and medical industries. Acetone (extra pure, 99.5% pure), silica gel (60–200 mesh, 99% pure), and aluminum oxide (Al_2O_3, active neutral) were purchased from LobaCheme Company.

Preparation of nZVI

For the synthesis of nZVI particles, about 2.1624 g $FeCl_3.6H_2O$ was dissolved in a 4/1 (v/v) ethanol/water mixture (96 mL ethanol + 24 mL deionized water) and efficiently stirred. Also, 0.1 molar $NaBH_4$ solution was prepared by mixing 1.5128 g $NaBH_4$ with 400 mL of deionized water. Excess borohydride was applied to ensure better formation of nZVI. The burette was filled with $NaBH_4$ solution and then adjusted to a flow rate of one drop per second. The burette was then fixed above the $FeCl_3.6H_2O$ solution placed in a magnetic stirrer. After the first drop of $NaBH_4$ into the $FeCl_3.6H_2O$ solution, black solid particles appeared immediately. Equation (1) shows the chemical reaction between sodium borohydride and iron chloride hexahydrate to form nZVI (Cumbal & SenGupta 2005). The stirring process was continued for another 10 min after adding the whole $NaBH_4$ solution. The black iron nanoparticles were separated from the liquid solution using a vacuum filtration technique. The prepared iron nanoparticles were filtered by placing them in two sheets of Whatman filter papers (42 circles, diameter 150 mm). To avoid rapid oxidation of the iron nanoparticles, they were washed three times with 50 mL of absolute ethanol. Finally, the prepared iron nanoparticles were dried in the oven overnight at 50°C. For storage purposes, a thin layer of ethanol was added above the iron nanoparticles to prevent the oxidation of iron.

$$2FeCl_3 + 6NaBH_4 + 18H_2O \rightarrow 2Fe^0 + 21H_2 + 6B[OH]_3 + 6NaCl \quad (1)$$

Characterization of nZVI

X-ray powder diffraction (XRD) was used for investigating the material structure of the prepared iron nanoparticles. A Philips XRD 3100 diffractometer (Philips Electronic Co., Eindhoven, The Netherlands) was used for conducting XRD analysis. It used a graphite monochromator and copper K-alpha radiation to produce X-rays with a wavelength of 1.5418 A°. The X-ray voltage was 40 mA, while the current value was 40 kV. The nZVI particles were placed in a stainless steel holder and scanned from 5° to 70° at a rate of 0.0167°/sec (Xi *et al.* 2010). Scanning the iron nanoparticles through a range of 2θ diffraction angle ensures all major kinds of iron and iron oxides are covered. The size of the iron nanoparticles was determined using an ultraviolet-visible spectrophotometer (UV/Vis). The surface structure of the prepared iron nanoparticles was observed before adsorption using a scanning electron microscope (SEM, Philips, Quanta 250 FEG, USA) at voltage 20 kV and magnification 120,000 x.

Batch experiments

The adsorption of BTEX onto nZVI was studied by the batch technique. A known weight of adsorbent (0.01, 0.016, 0.022, and 0.028 g/L) of nZVI was equilibrated with 100 mL of the aqueous BTEX solution of known concentration (36, 24 and 12 µg/L) in 250 mL Erlenmeyer flasks and shaken at 100, 200, and 300 rpms at temperatures of 30, 40, 50, and 60°C. The removal efficiency for BTEX was studied at pH 4, 5, 6, 7, 8 and 9. All experiments were repeated three times and the average values were recorded. Blank samples that only contain BTEX compounds without adding any adsorbent were run along with the samples containing nZVI. Instruments and tools used in this study were calibrated prior to the experiment.

After equilibration, Whatman No. 42 filter paper was used to separate the suspension part of the adsorbent from the solution. Then, the concentration of BTEX remaining in solution was measured using a Master DANI GC (fast gas chromatograph) using a micro column DN5 non-polar diameter 60 m × 0.32 μm × 0.25 mm, wool liner 2 mm, split/split less injector and FID detector according to ASTM 2005 standard method for water and wastewater (Water Environment Federation & American Public Health Association 2005). The percentage of BTEX compounds removal was calculated using Equation (2). The amount of BTEX absorbed by weight of nZVI was calculated using Equation (3).

$$\text{Sorption}\,[\%] = \left[\frac{C_o - C_e}{C_o}\right] \times 100 \tag{2}$$

where C_o is the initial concentration of BTEX compounds in solution (μg/L) and C_e is the equilibrium concentration of BTEX compounds in solution (μg/L)

$$q_e = \frac{[[C_o - C_e]V]}{m} \tag{3}$$

where q_e is the equilibrium adsorption capacity (μg/g), V is the volume of aqueous solution (L), and m is the dry weight of the adsorbent (g).

Artificial neural network

ANN structure

A neural network composed of three layers: input, hidden, and output, was structured to predict the removal efficiency of BTEX. The input layer receives data from six experimental parameters; temperature, stirring rate, initial BTEX concentration, contact time, pH, and adsorbent dose. Ten neurons were included in the hidden layer, and thus the structure used for the prediction of BTEX removal efficiency was 6 – 10 – 1 (Figure 1). A trial and error procedure allows the estimation of the actual numbers of neurons and hidden layers. Target and input vectors were divided into three groups: 60% of the data were used for training the network; 20% of the data were used for model validation; 20% were used for testing the created network.

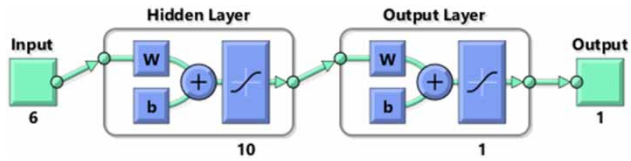

Figure 1 | ANN of 6 – 10 – 1 structure used for the prediction of BTEX removal efficiency.

ANN properties

The data in this study were classified using a feedforward backpropagation algorithm. In this algorithm, the mean squared error (MSE) is calculated for the purpose of comparing the target data with the output data (Equation (4)). The values of the biases and weights are adjusted by propagating the MSE back from the output layer to the input layer until the maximum number of iterations is reached.

$$\text{MSE} = \frac{\sum_{i=1}^{N}(t_i - a_i)^2}{N} \tag{4}$$

where N is the number of measured data, and a_i and t_i are predicted output and the target, respectively.

The Levenberg–Marquartd method (trainlm) was used for network training. The 'purlin' (Equation (5)) and 'tansig' (Equation (6)) transfer functions were chosen for the output layer and hidden layer, respectively. By employing the 'tansig' function, the output is limited between −1 and +1 and the neuron's net input can have any value between positive and negative infinity. The 'tansig' function is mainly used for pattern recognition, while the 'purlin' function was used for function fitting.

$$f(x) = x, \; -\infty < f(x) < +\infty \tag{5}$$

$$f(x) = \frac{e^x - e^{-x}}{e^x + e^{-x}}, \; -1 \le f(x) \le 1 \tag{6}$$

RESULTS AND DISCUSSION

Characterization of nZVI

The XRD pattern as shown in Figure 2(a) shows two peaks at $2\theta = 44.58°$ and 64.99° that fit well with the body-centered

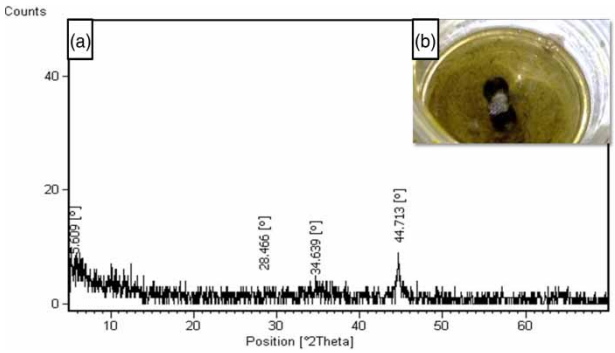

Figure 2 | (a) X-ray powder diffraction results, (b) magnetic properties of iron.

structure that represent the Fe (110) and Fe (200) planes, respectively. By analyzing the positions and the shape of the diffraction peaks, the Scherrer formula can be used to calculate the average grain size of crystallites (Equation (7)):

$$D = \frac{k\lambda}{\beta \cos \theta} \tag{7}$$

where D is the crystallite size (nm), β is the full wave at half maximum (FWHM) (0.0067 and 0.002898 radian for 2θ 44.713 and 64.9°, respectively), θ is the diffraction angle, k is the Scherrer constant (0.9), and λ is the x-ray wavelength.

The calculated particle size ranged from 23 to 59 nm which is in good agreement with the result obtained from the SEM analysis. The XRD analysis also proved that there is no formation of iron oxide and the nZVI was predominantly present in the sample. Figure 2(b) shows that the magnet attracts the metals which indicates the formation of iron nanoparticles. This result agrees with Zhang *et al.* (2004) on preparing nZVI. The results of UV-visible spectroscopy also indicated the formation of iron nanoparticles with particle size ranging from 20 to 60 nm, where the two absorption peaks were recorded at 193 and 194 nm and one peak was recorded at 211 nm, as shown in Figure 3(a). This result agrees with Abdel-Gawad *et al.* (2016) on preparing nZVI. Figure 3(b) shows the SEM image of the prepared nZVI particles before treatment. The prepared iron nanoparticles formed large nanoclusters due to magnetic forces between the iron nanoparticles. The nZVI particles also formed an irregular surface structure with an average size of 50 nm. Many pores were observed which allows better mass transfer and diffusion of BTEX compounds to the inner iron nanoparticles (Shih *et al.* 2011).

Removal of BTEX compounds using nZVI

Effect of contact time

The effect of contact time on BTEX removal was studied at 15, 30, 45 and 60 min. An initial BTEX mixture concentration of 12 μg/L was used along with 0.22 g of nZVI added to 1,000 mL of total BTEX mixture. The stirring rate was fixed at 100 rpm using a horizontal shaker. The pH was adjusted to 7 ± 0.2 and the temperature to 40 ± 3°C.

As shown in Figure 4(a), the removal efficiency of each BTEX compound and the BTEX mixture increased with increasing contact time. The removal of the BTEX mixture increased from 90.17% (recorded after 15 mins of contact time) to 97.67% (recorded after 60 mins of contact time).

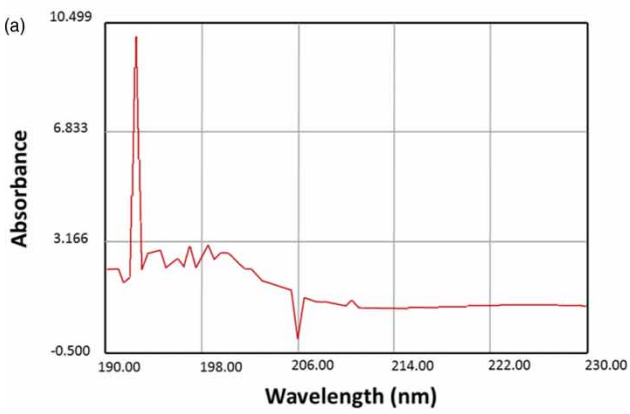

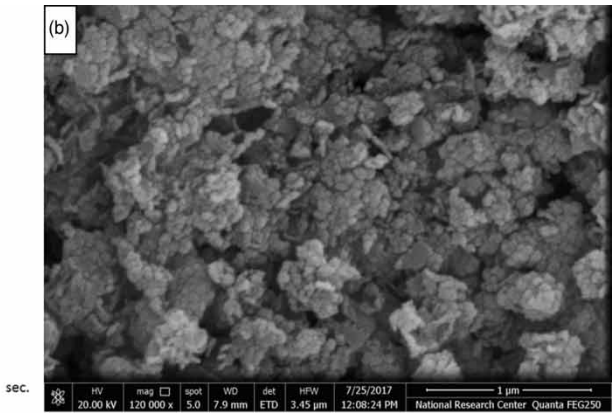

Figure 3 | (a) UV visible spectrum of the iron nanoparticles, (b) SEM analysis.

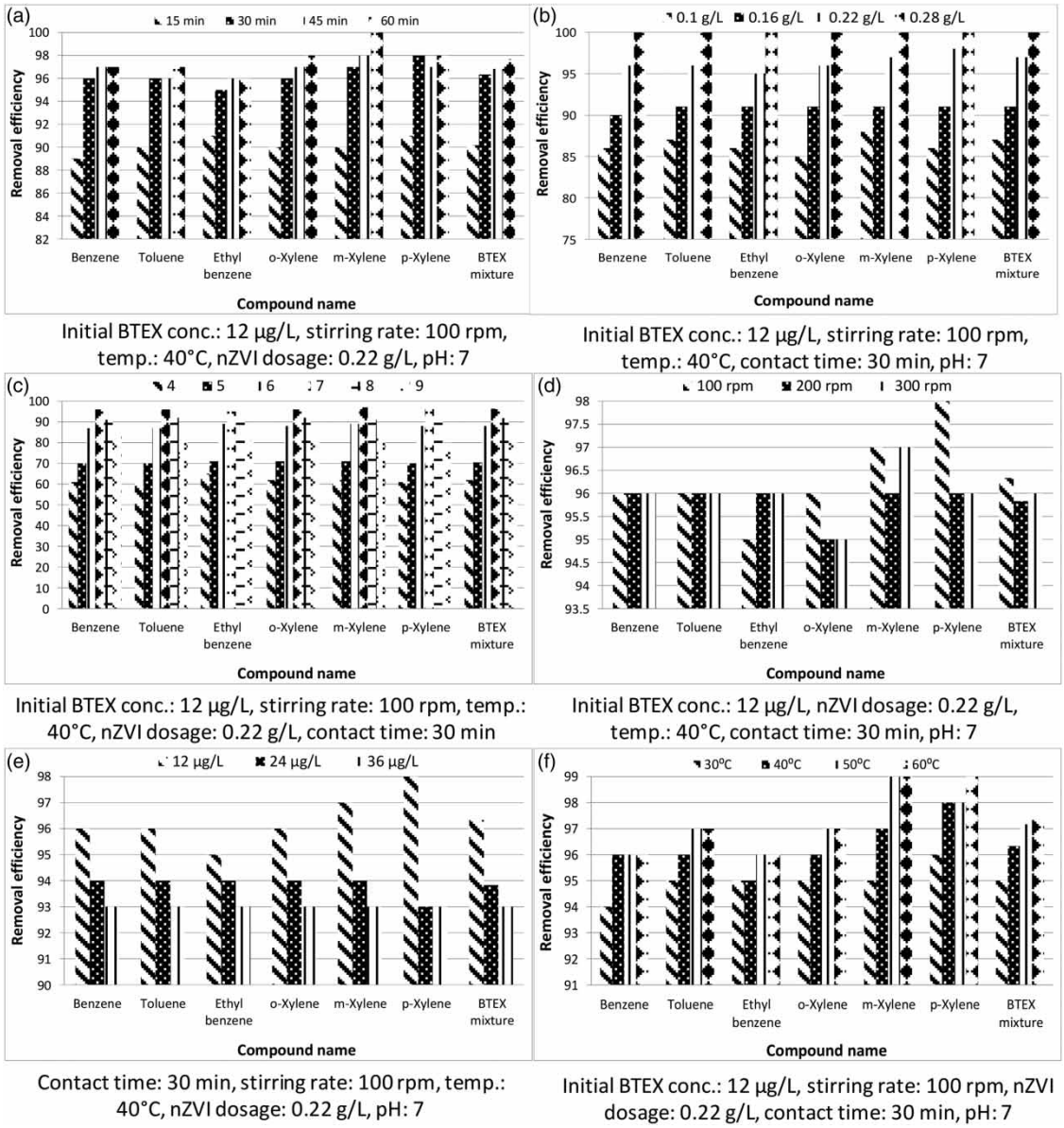

Figure 4 | Effect of experimental factors on removal efficiency of BTEX using nZVI: (a) contact time, (b) nZVI dosage, (c) pH, (d) stirring rate, (e) initial BTEX concentration, and (f) temperature.

At time zero the concentrations of BTEX compounds were distributed equally in the solution, and by adding the nZVI dosage into the solution the excess amount of $NaBH_4$ which covers the nZVI particles dissolved in the solution leaving bare nZVI to react with water. The pH of the solution tends to be gradually alkaline and the BTEX compounds adsorb onto the surface of the iron nanoparticles gradually until reaching saturation point. A 7% increase in the removal efficiency was recorded after increasing the contact time from 15 to 30 min, while only 1% increase was recorded after increasing the contact time from 30 to 60 min due to coming close to saturation. The high removal efficiency in the first 30 min of the reaction is attributed to intermolecular forces that hold the adsorbate in contact with adsorbent surfaces through the ready-to-adsorb and empty binding sites (Mohammadi *et al.* 2017).

A contact time of 30 min was selected for this study since the rate of BTEX removal was almost stable for contact times above 30 min. These results agree with El-Shafei *et al.* (2016) who addressed the removal of BTEX using entrapped nZVI in alginate polymer, and they concluded that the optimum contact time ranged from 30 to 45 min. The obtained results also showed that the removal efficiencies for xylene and toluene are higher than the removal efficiencies for ethylbenzene and benzene, as shown in Figure 4(a). This is mainly due to the mechanism of BTEX sequestration by nZVI, where sometimes the degradation process becomes more effective than the adsorption process leading to an increase in benzene concentration in the solution. In this case the degradation process for toluene and xylene through the free electrons is normally followed by the adsorption process. However, if the adsorption process is more effective than the degradation process, the adsorption of benzene will be easier than the other BTEX compounds and the removal efficiency will give similar results for all BTEX compounds.

Effect of adsorbent dose

The effect of the adsorbent dose was studied at 0.1, 0.16, 0.22, and 0.28 g/L. The nZVI was added to 1,000 mL of total BTEX mixture at a concentration of 12 μg/L for 30 min at pH 7.0 ± 0.2 and temperature 40 ± 3°C. The stirring rate was fixed at 100 rpm.

The removal efficiency of each BTEX compound and the BTEX mixture increased with the increase of the adsorbent dose, as shown in Figure 4(b). The removal of the BTEX mixture increased from 86.33% (nZVI dose of 0.1 g/L) to 100% (nZVI dose of 0.28 g/L). This means that the BTEX removal efficiency is directly proportional to nZVI dosage. An increase in nZVI dosage resulted in an increase in the number of adsorption sites which in turn allowed the adsorption of a greater amount of BTEX compounds. As shown in Figure 4(b), the removal efficiency at different adsorbent doses was similar for all BTEX compounds which probably means that the adsorption process was more effective than the degradation process. As shown in Figure 5, the uptake rate decreased with the increase in the adsorbent dose, but the uptake rate decreased at a fast rate when the dose increased from 0.1 to 0.16 g/L, and then decreased at a slow rate when the dose increased from 0.16 to 0.28 g/L. Therefore, an adsorbent dose of 0.16 g/L was selected for this study.

Effect of pH

The effect of pH on the BTEX removal was studied at pH values above and below the point of zero charge (PZC). The PZC for nZVI is around 7.7 (Prabu & Parthiban 2013). The nZVI is well known to be ineffective at high pH values due to the presence of iron oxide (Bezbaruah *et al.* 2011). The removal efficiency for BTEX was studied at pH

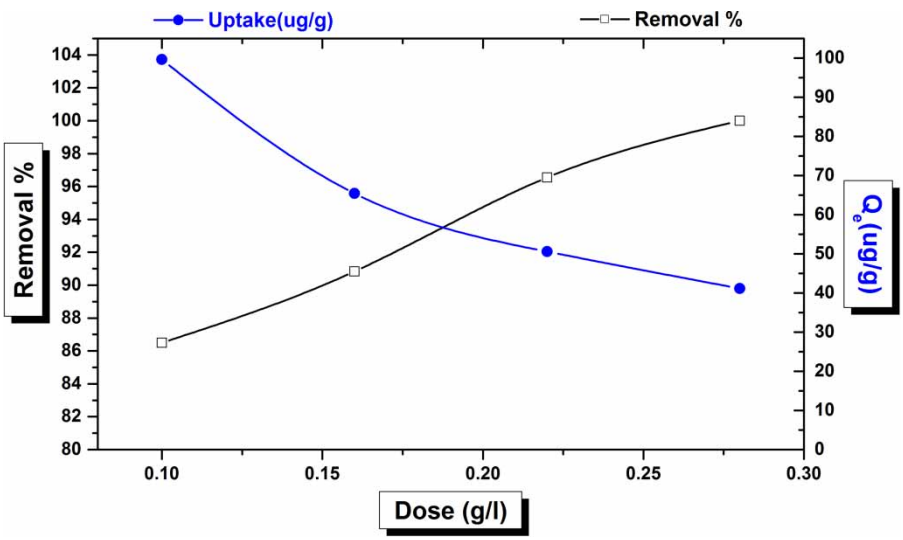

Figure 5 | Minimum effective dose for BTEX mixture removal using nZVI.

4, 5, 6, 7, 8 and 9. The pH was adjusted using H_2SO_4 to provide acidic media, and NaOH to provide an alkaline media. About 0.22 g nZVI was added to 1,000 mL of total BTEX mixture at a concentration of 12 μg/L for 30 min at temperature 40 ± 3°C. The stirring rate was fixed at 100 rpm.

The removal efficiency of each BTEX compound and the BTEX mixture increased at a fast rate in the acidic media and reached the highest value at pH 7, as shown in Figure 4(c). The removal of the BTEX mixture increased from 62% at pH 4 to 96.3% at pH 7. This means that in the acidic media the solubility of some nZVI particles in the acidic solution led to a decrease in sorbent capacity. Additionally, in the acidic media, the efficiency of the BTEX compounds degradation has decreased because some of the free electrons generated by nZVI have combined with excess H^+ found in the solution forming water. In a neutral solution there is excess of OH^- that can be effective in the removal of BTEX compounds. Above pH 7, however, the effect was reversed, and the removal efficiency decreased with increasing pH value, decreasing to 81.33% at pH 9. This means that in the alkaline media the excess of hydroxyl ions in the solution compete with negative ions on the nZVI surface which decreases the adsorption process. These results agree with Seifi *et al.* (2011) who addressed the removal of BTEX using surfactant-modified natural zeolite, and they concluded that the optimum pH was between 6 and 8. Figure 4(c) shows that the removal efficiency at different pH values was similar for all BTEX compounds which probably means that the benzene was easy to absorb, and the adsorption process was more effective than the degradation process.

Effect of stirring rate

The effect of the stirring rate on the BTEX removal was studied at 100, 200, and 300 rpm using a horizontal shaker. An initial BTEX mixture concentration of 12 μg/L was used along with 0.22 g of nZVI added to 1,000 mL of total BTEX mixture for 30 min. The pH was adjusted to 7 ± 0.2 and the temperature to 40 ± 3°C.

The removal efficiency of the BTEX mixture was recorded as 97% for a stirring rate of 100 rpm and then the removal efficiency decreased at a slow rate for stirring rates higher than 100 rpm, as shown in Figure 4(d). This may be attributed to the disturbance that may occur to the system which may weaken electrostatic forces and thus affect the attachment mechanism (Djenouhat *et al.* 2008). This result is in good agreement with the results obtained from the isotherm study which indicated that the Freundlich isotherm is more appropriate in explaining the adsorption capacity. Based on the Freundlich theory, the physical adsorption that binds the BTEX group with nZVI is characterized by a weak bond which increases the possibility of BTEX compounds separating from the nZVI surface. These results also agree with Seifi *et al.* (2011) who addressed the removal of BTEX using granulated surfactant-modified natural zeolite nanoparticles, and they concluded that the suitable stirring rate for the best removal of BTEX compounds was between 100 and 200 rpm. In general, there is no big variation in the BTEX mixture removal efficiencies with a change in stirring rates and this mainly due to the high efficiency of the iron nanoparticles and their ability to diffuse in all the solution without the need for a high stirring rate. Figure 4(d) shows that the removal efficiency at different stirring rates was similar for all BTEX compounds which probably means that the adsorption process was more effective than the degradation process.

Effect of the initial BTEX concentration

The effect of the initial BTEX mixture concentration was studied at concentrations of 12, 24, and 36 μg/L, these concentrations were suggested according to the likely occurrence and limits set by WHO for drinking water. About 0.22 g nZVI was added to 1,000 mL of total BTEX mixture for 30 min. The pH was adjusted to 7 ± 0.2 and the temperature to 40 ± 3°C. The stirring rate was fixed at 100 rpm.

The removal efficiency of each BTEX compound and the BTEX mixture decreased with the increase in the initial BTEX concentration because the iron nanoparticles reached their maximum adsorption capacity, as shown in Figure 4(e). At low BTEX mixture concentrations, all BTEX compounds are adsorbed by nZVI because the number of surface active sites is higher than the total BTEX compounds in the solution (Petala *et al.* 2013). The removal of the BTEX mixture decreased from 96.33% at an initial BTEX mixture concentration of 12 μg/L to 93% at an initial concentration of 36 μg/L. This means that at high initial BTEX concentration, fewer adsorption sites were available to adsorb all the contaminants in the solution. Additionally, the competition between the BTEX compounds increases on the

nZVI surface, which decreases the adsorption capacity. Figure 4(e) shows that the removal efficiency at different BTEX concentrations was similar for all BTEX compounds which probably refers to a highly effective adsorption performance of the iron nanoparticles.

Effect of temperature

The effect of temperature was studied at 30, 40, 50, and 60°C. About 0.22 g nZVI was added to 1,000 mL of total BTEX mixture at a concentration of 12 μg/L for 30 min. The pH was adjusted to 7 ± 0.2 and the stirring rate was fixed at 100 rpm. The removal efficiency of each BTEX compound and the BTEX mixture increased with the increase in temperature because increasing the temperature enhances the interaction between nZVI and BTEX through increasing BTEX solubility in aqueous solution, and decreasing the amount of dissolved oxygen in the solution to prevent nZVI oxidation. The increase in BTEX removal efficiency with increasing temperature may also be attributed to the decrease in the activation energy barrier, as well as the creation of some adsorption sites (Shukla *et al*. 2002; Karthikeyan *et al*. 2005). The adsorption process in this case is probably endothermic (Bulut & Aydın 2006). As shown in Figure 4(f), the removal of the BTEX mixture increased from 95% at a temperature of 30°C to 97.33% at a temperature of 60°C. These results agree with Seifi *et al*. (2011) who addressed the removal of petroleum aromatic hydrocarbons using surfactant-modified natural zeolite, and they concluded that the removal efficiency decreased significantly from 93% to 10% when the temperature decreased from 20°C to 4°C. Figure 4(f) shows that there is no big difference in the removal efficiency at the different temperatures studied for all BTEX compounds.

Adsorption isotherm study for BTEX removal using nZVI

An adsorption isotherm study was used to predict and evaluate the sorption capacity of a sorbent. This equilibrium study was described by measuring the amount of solute adsorbed per unit weight of the iron nanoparticles, as well as the concentration of solute remaining in solution (Nkansah 2012). The most commonly used isotherm models for wastewater and water treatment applications are the Freundlich and the Langmuir equations. The Langmuir isotherm model assumes monolayer adsorption over a homogeneous adsorbent surface. The linearized form of the Langmuir model is given in Equation (8). The plot of C_e versus C_e/q_e is employed to generate the values of K_L and q_{max}. The Freundlich isotherm describes a heterogeneous multilayer adsorption surface and can be determined using Equation (9), where K_f and n can be evaluated by plotting $\ln(q_e)$ and $\ln(C_e)$.

$$\frac{C_e}{q_e} = \frac{1}{K_L q_{max}} + \frac{C_e}{q_{max}} \tag{8}$$

where q_e is the amount of BTEX adsorbed by the biomass at equilibrium (μg/g), C_e is the BTEX concentration in the solution at equilibrium (μg/L), q_{max} is the maximum monolayer adsorption capacity (μg/g), and K_L is the Langmuir constant (L/μg).

$$\ln(q_e) = \ln(K_f) + \left(\frac{1}{n}\right) \ln(C_e) \tag{9}$$

where K_f is the Freundlich constant related to adsorption capacity ((μg/g)(μg/L) − 1/n) and n is the Freundlich constant related to adsorption intensity (dimensionless).

The Freundlich isotherm model with sum of squares differences (SSD) between modeling and experimental results for all BTEX compounds ranging from 0.0055 to 1.377 showed a better fit with the adsorption data than the Langmuir isotherm model with SSD ranging from 0.0788 to 6.729, as shown in Table 1. The agreement of the Freundlich isotherm results with the experimental data indicated that multilayer adsorption has occurred. This indicates that the Freundlich constants are more appropriate in explaining the adsorption

Table 1 | Isotherm study for adsorption of BTEX onto nZVI

Isotherm study	Compound	q_{max}, μg/g	K_L, L/μg	SSD
Langmuir	Benzene	6.3	22.519	0.0788
	Toluene	66.75	1.838	1.282
	Ethyl benzene	81.436	1.332	1.565
	o-Xylene	53.62	2.635	4.989
	m-Xylene	43.647	4.1347	6.729
	p-Xylene	5.67	75.61	0.243
Freundlich	Compound	1/n, L/g	K_F, (μg/g) (μg/L) − 1/n	SSD
	Benzene	0.219	7.097	0.0055
	Toluene	0.708	54.74	0.134
	Ethyl benzene	0.759	57.197	0.427
	o-Xylene	0.641	50.132	1.377
	m-Xylene	0.566	46.6946	1.042
	p-Xylene	0.136	6.3724	0.1037

capacity. The high values of K_f which ranged from 6.3724 to 57.197 μg/g indicate that the iron nanoparticles have a high ability to adsorb BTEX compounds. The value of $1/n$ (ranging from 0.136 to 0.759 L/g) was located between 0 and 1, which indicates that the biosorption of BTEX compounds onto iron nanoparticles was favorable under the studied conditions. These results agree with Simantiraki *et al.* (2013) who addressed the removal of BTEX from groundwater using sewage sludge and municipal solid waste compost, and they concluded that the Freundlich isotherm model showed the best fit compared to the other models.

Artificial neural network

Adjusted weights and biases

A weight matrix ($W_{10\times6}$) was generated by connecting each element of the input vector ($P_{6\times1}$) to each hidden layer neuron. A net input was a result of summing up the weighted inputs ($\Sigma W_{10\times6}.P_{6\times1}$) and adding a 10-length bias ($b_{10\times1}$). The 'tansig' function was then used to transfer the calculated net input ($u_{10\times1} = \Sigma W_{10\times6}.P_{6\times1} + b_{10\times1}$) to the output layer.

A weight matrix ($W_{1\times10}$) was generated by connecting each hidden layer neuron ($P_{10\times1}$) to the output layer single neuron. A net input was a result of summing up the weighted inputs ($\Sigma W_{1\times10}.P_{10\times1}$) and adding a 1-length bias ($b_{1\times1}$). The 'purlin' function was then used to transfer the calculated net input ($u_{1\times1} = \Sigma W_{1\times10}.P_{10\times1} + b_{1\times1}$) to the output layer.

$$W_{1\times10} = \begin{bmatrix} -2.3994 & 0.0079141 & 2.2102 & -0.49991 \\ -0.82658 & -1.7344 & -0.18274 & 0.68991 \\ -0.36944 & 0.71702 & & \end{bmatrix}$$

$$b_{1\times1} = [-0.57835]$$

Training performance

The results of the training step such as the number of validation checks and the gradient magnitude were 6 and 0.1336, respectively. Although the gradient magnitude was higher than 1e-5 (least error level), the training step was terminated due to reaching the maximum number of validation checks at epoch 6, as shown in Figure 6.

Validation performance

The plot in Figure 7 shows the relationship between the iteration number and the mean square error (MSE) performance. The MSE of the training step decreased gradually and reached the lowest value at epoch number 6. This trend is normal and does not represent a problem in the training step. On the other hand, the MSE of the validation

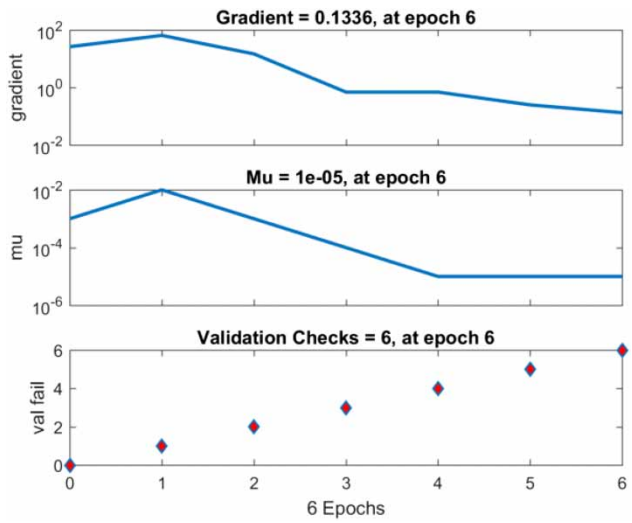

Figure 6 | Training performance for the prediction of BTEX removal efficiency using ANN.

$$W_{10\times6} = \begin{bmatrix} 1.0788 & 0.12317 & -3.2612 & 0.71537 & -1.3651 & 0.37869 \\ 0.34562 & -0.14639 & 0.83266 & 1.0134 & -0.75519 & 1.1897 \\ 0.60646 & 2.8405 & -1.0796 & -0.45097 & 0.20113 & -0.63812 \\ 1.0953 & 0.66059 & 0.34827 & -1.4306 & -0.66884 & -0.45845 \\ 1.3884 & -0.04435 & 2.1729 & -0.8727 & 0.54874 & -0.6418 \\ 0.031463 & 0.29378 & -2.5981 & 0.51566 & 0.69181 & 0.11458 \\ -0.26534 & -0.82474 & -0.35934 & 1.7009 & 0.66876 & 0.5474 \\ 0.43573 & 0.55404 & 0.42397 & 0.63472 & 0.070405 & 1.101 \\ -1.4838 & -0.099917 & 0.17592 & -2.0955 & -1.3881 & -1.0086 \\ -0.88494 & -0.35335 & 0.06749 & 1.4176 & 1.4829 & -0.72206 \end{bmatrix} \quad b_{10\times1} = \begin{bmatrix} -1.595 \\ -1.854 \\ -1.476 \\ 0.8114 \\ -0.063 \\ -0.614 \\ -1.070 \\ 1.3012 \\ -1.198 \\ -2.414 \end{bmatrix}$$

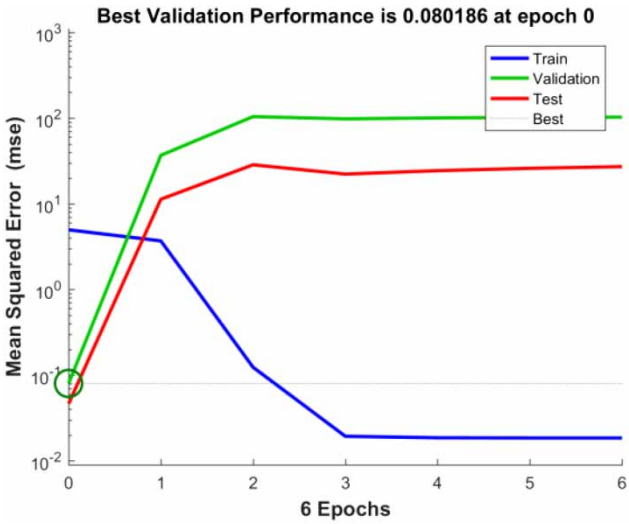

Figure 7 | Best validation performance for the prediction of BTEX removal efficiency using ANN.

step increased gradually after epoch number 0, indicating that the model is overfitting the data. The test and validation curves were similar in behavior and they increased with the number of epochs. In summary, the best validation performance was 0.080186 at epoch 0.

Regression plot

The coefficient of determination (r^2-value) between network targets and network outputs is depicted in Figure 8. The solid line represents the best-fitting line, while the dashed line signifies the perfect result. A good fit between the output and the target data was observed for training, validation and test steps with r^2-values of 0.95932, 0.84235, and 0.99996, respectively. The overall r^2-value considering the three steps was 0.97064, indicating the model reliability. This means that 97.06% of the variations in BTEX removal efficiency were explained by the studied parameters. Consequently, the proposed ANN was able to accurately estimate the removal efficiency for BTEX in the studied range.

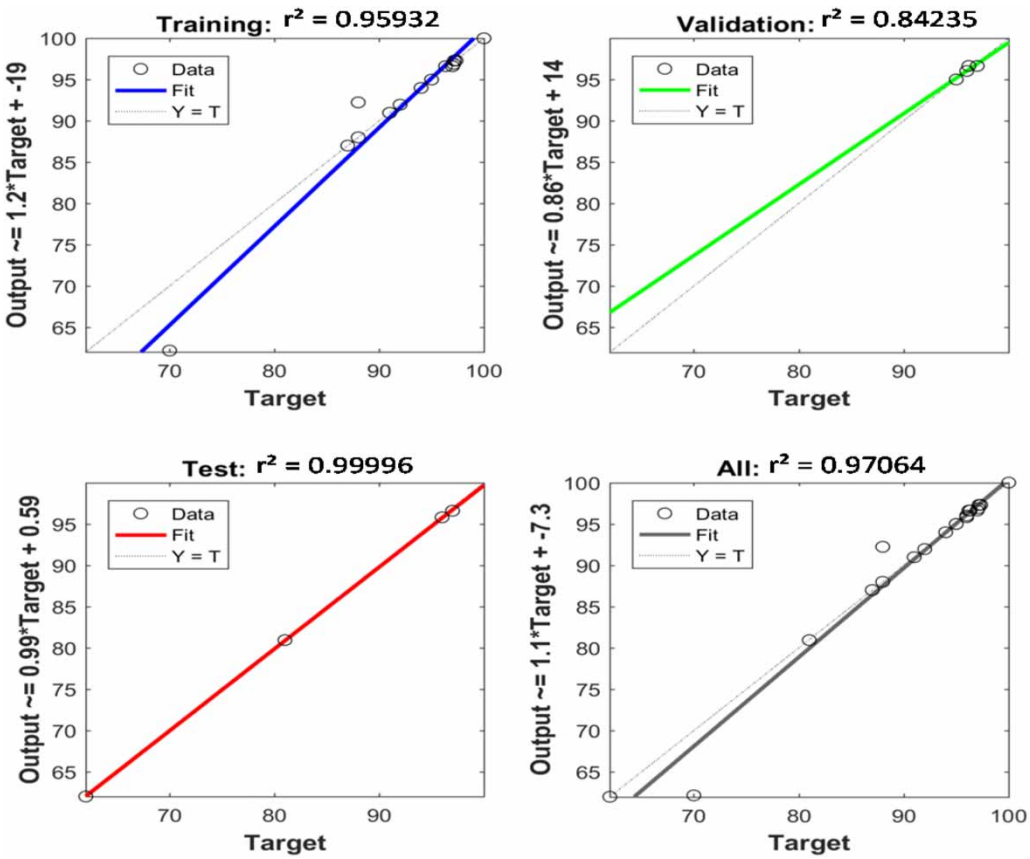

Figure 8 | Regression plot between target and output for the prediction of BTEX removal efficiency using ANN.

Model verification and optimization

In order to confirm the validity of the predicted model, a comparison was conducted between the experimental results and the outputs of the model by calculating the average absolute error for 24 solutions. The ANN model was found to be reliable in predicting the removal efficiency of BTEX, where the average absolute error of BTEX removal efficiencies for 24 experimental runs was 0.6272%.

Cost estimation

The capital and operating costs of BTEX removal by nZVI was estimated under the optimal environmental conditions. The construction cost of the adsorption unit was estimated by multiplying the adsorption unit capacity by the construction cost of 1 m^3. The adsorption unit capacity was estimated using Equation (10) (Alalm *et al.* 2015).

$$C = \frac{t_t}{t_w} \times \frac{V_t}{D} \tag{10}$$

where C is the adsorption unit capacity (m^3), t_t is the batch treatment time (min), t_w is the working time per day (min), V_t is the wastewater discharge in a year (m^3/year), and D is the number of operating days per year (1/year).

The operating cost for each cubic meter (USD/m^3) was calculated by summing up the cost of the nZVI and the utilized energy cost (stirring and cleaning). The nZVI cost was calculated by multiplying the nZVI dosage of 0.22 g/L by the unit price of 0.015 USD/g which gives 0.0033 USD/L (3.3 USD/m^3).

The utilized energy to treat 1 cubic meter was calculated by applying the electricity tariff of 0.075 USD/kWh (Nasr *et al.* 2013). The estimated energy cost was 0.2 USD/m^3. The total cost can be calculated by summing up these two costs which gives 3.5 USD/m^3. This result revealed that nZVI seems to be a better alternative to other treatment technologies due to its low production cost.

CONCLUSIONS

The results of the batch studies indicated that iron nanoparticles are effective in BTEX removal under specific conditions. The removal efficiency of the BTEX mixture increased with the increase of the adsorbent dose, contact time, and temperature, while a decrease in the removal efficiency was recorded with the increase in stirring rate and initial BTEX concentration. The removal efficiency of BTEX mixture decreased for pH values below or above the neutral pH value. The best BTEX removal was achieved using 0.22 g nZVI at pH ranging from 6 to 8, a stirring rate of 100 rpm, temperature of 60°C, and contact time of 30 minutes. The highest removal efficiency was also achieved at an initial BTEX concentration of 12 μg/L. The removal efficiency of all BTEX compounds was similar under the same conditions which probably means that the adsorption process was more effective than the degradation process. The isothermal data showed that the Freundlich isothermal was the best fitting model with SSD for the six BTEX compounds ranging from 0.0055 to 1.377 when compared to the Langmuir isothermal model with SSD ranging from 0.0788 to 6.729, which indicated that a multilayer adsorption had occurred. Modeling results showed that ANN was reliable in predicting BTEX removal efficiency under the tested experimental conditions with an r^2-value of 0.97064. This study also indicated that iron nanoparticles could be employed as an efficient and cost-effective adsorbent for the removal of BTEX compounds. Under the optimal conditions, it is estimated that the cost of BTEX removal by nZVI will be about 3.5 USD per cubic meter.

ACKNOWLEDGEMENTS

This work was supported by the Egyptian Housing Building Research Center (HBRC).

REFERENCES

Abdel-Gawad, S. A., Baraka, A. M., El-Shafei, M. M. & Mahmoud, A. S. 2016 Effects of nano zero valent iron and entrapped nano zero valent iron in alginate polymer on poly aromatic hydrocarbons removal. *Journal of Environment & Biotechnology Research* **5** (1), 18–28.

Alalm, M., Tawfik, A. & Ookawara, S. 2015 Degradation of four pharmaceuticals by solar photo-Fenton process: kinetics and costs estimation. *J. Environ. Chem. Eng.* **3** (1), 46–51.

Bezbaruah, A. N., Shanbhogue, S. S., Simsek, S. & Khan, E. 2011 Encapsulation of iron nanoparticles in alginate biopolymer for trichloroethylene remediation. *Journal of Nanoparticle Research* **13** (12), 6673–6681.

Bulut, Y. & Aydın, H. 2006 A kinetics and thermodynamics study of methylene blue adsorption on wheat shells. *Desalination* **194**, 259–267. doi: 10.1016/j.desal.2005.10.032.

Crosse, M., Anderson, B., Doran, K., Bogart, G., Desaulniers, H., Hamann, C., Organek, D., Price, R., Ritchie, C. & Ryba, S. 2007 *Defense Health Care: Activities Related to Past Drinking Water Contamination at Marine Corps Base Camp Lejeune.* DTIC Document, Washington, DC, USA.

Cumbal, L. H. & SenGupta, A. K. 2005 Preparation and characterization of magnetically active dual-zone sorbent. *Industrial & Engineering Chemistry Research* **44** (3), 600–605.

Davidson, J. M. & Creek, D. N. 2000 Using the gasoline additive MTBE in forensic environmental investigations. *Environmental Forensics* **1** (1), 31–36.

Djenouhat, M., Hamdaoui, O., Chiha, M. & Samar, M. H. 2008 Ultrasonication-assisted preparation of water-in-oil emulsions and application to the removal of cationic dyes from water by emulsion liquid membrane part 2. Permeation and stripping. *Separation and Purification Technology* **63**, 231–238. doi: 10.1016/j.seppur.2008.05.005.

Edil, T. B. 2003 A review of aqueous-phase VOC transport in modern landfill liners. *Waste Management* **23** (7), 561–571.

El-Shafei, M. M., Mahmoud, A. S., Mostafa, M. K. & Peters, R. W. 2016 Effects of entrapped nZVI in alginate polymer on BTEX removal. In: *AIChE Annual Meeting*, San Francisco, CA, November 13–18.

Falta, R. W., Bulsara, N., Henderson, J. K. & Mayer, R. A. 2005 Leaded-gasoline additives still contaminate groundwater. *Environmental Science & Technology* **39** (18), 378A-384A.

Gautam, R. K. & Chattopadhyaya, M. C. 2017 *Advanced Nanomaterials for Wastewater Remediation.* Taylor & Francis Group, Boca Raton, FL.

Giasuddin, A. B. M., Kanel, S. R. & Choi, H. 2007 Adsorption of humic acid onto nanoscale zerovalent iron and its effect on arsenic removal. *Environmental Science & Technology* **41** (6), 2022–2027. doi:10.1021/Es0616534.

Gorelick, S. M. & Gvirtzman, H. 1995 In-situ vapor stripping for removing volatile organic compounds from groundwater. US Patent 5,389,267.

Kampa, M. & Castanas, E. 2008 Human health effects of air pollution. *Environmental Pollution* **151** (2), 362–367.

Karthikeyan, T., Rajgopal, S. & Miranda, L. R. 2005 Chromium (VI) adsorption from aqueous solution by Hevea Brasilinesis sawdust activated carbon. *Journal of Hazardous Materials* **124** (1–3), 192–199. doi: 10.1016/j.jhazmat.2005.05.003.

LaGrega, M., Buckingham, P. & Evans, J. 2001 *Hazardous Waste Management, Chapter 9: Physicochemical Processes*. McGraw-Hill, New York, NY.

Lee, S., Chiu, M., Ho, K., Zou, S. & Wang, X. 2002 Volatile organic compounds (VOCs) in urban atmosphere of Hong Kong. *Chemosphere* **48** (3), 375–382.

Mazzeo, D. E. C., Fernandes, T. C. C. & Marin-Morales, M. A. 2011 Cellular damages in the Allium cepa test system, caused by BTEX mixture prior and after biodegradation process. *Chemosphere* **85** (1), 13–18.

Mohammadi, L., Bazrafshan, E., Noroozifar, M., Ansari-Moghaddam, A., Barahuie, F. & Balarak, D. 2017 Adsorptive removal of Benzene and Toluene from aqueous environments by cupric oxide nanoparticles: kinetics and isotherm studies. *Journal of Chemistry*. doi:10.1155/2017/2069519.

Moran, M. J., Zogorski, J. S. & Squillace, P. J. 2007 Chlorinated solvents in groundwater of the United States. *Environmental Science & Technology* **41** (1), 74–81.

Nasr, M., Tawfik, A., Ookawara, S. & Suzuki, M. 2013 Environmental and economic aspects of hydrogen and methane production from starch wastewater industry. *J. Water Environ. Technol.* **11** (5), 463–475.

Nkansah, M. A. 2012 *Environmental Remediation: Removal of Polycyclic Aromatic Hydrocarbons*. Dissertation, The University of Bergen, Norway.

Petala, E., Dimos, K., Douvalis, A., Bakas, T., Tucek, J., Zbořil, R. & Karakassides, M. A. 2013 Nanoscale zero-valent iron supported on mesoporous silica: characterization and reactivity for Cr(VI) removal from aqueous solution. *Journal of Hazardous Materials* **261**, 295–306. doi: 10.1016/j.jhazmat.2013.07.046.

Prabu, D. & Parthiban, R. 2013 Synthesis and characterization of nanoscale zero valent iron (NZVI) nanoparticles for environmental remediation. *Asian Journal of Pharmacy and Technology* **3** (4), 181–184.

Pronczuk, J. & Surdu, S. 2008 Children's environmental health in the Twenty-First Century. *Annals of the New York Academy of Sciences* **1140** (1), 143–154.

Rahman, N., Abedin, Z. & Hossain, M. A. 2014 Rapid degradation of azo dyes using nano-scale zero valent iron. *American Journal of Environmental Sciences* **10** (2), 157.

Raychoudhury, T. & Scheytt, T. 2013 Potential of zerovalent iron nanoparticles for remediation of environmental organic contaminants in water: a review. *Water Science and Technology* **68** (7), 1425–1439.

Seifi, L., Torabian, A., Kazemian, H., Bidhendi, G. H., Azimi, A. A., Nazmara, S. & AliMohammadi, M. 2011 Adsorption of BTEX on surfactant modified granulated natural zeolite nanoparticles: parameters optimizing by applying taguchi experimental design method. *Clean – Soil, Air, Water* **39** (10), 939–948.

Shih, Y., Hsu, C. & Su, Y. 2011 Reduction of hexachlorobenzene by nanoscale zero-valent iron: kinetics, pH effect, and degradation mechanism. *Sep. Purif. Technol.* **76** (3), 268–274. doi: 10.1016/j.seppur.2010.10.015.

Shukla, A., Zhang, Y. H., Dubey, P., Margrave, J. L. & Shukla, S. S. 2002 The role of sawdust in the removal of unwanted materials from water. *Journal of Hazardous Materials* **95** (1–2), 137–152. doi: 10.1016/S0304-3894(02)00089-4.

Simantiraki, F., Kollias, C. G., Maratos, D., Hahladakis, J. & Gidarakos, E. 2013 Qualitative determination and application

of sewage sludge and municipal solid waste compost for BTEX removal from groundwater. *Journal of Hazardous Materials* **1** (1–2), 9–17. doi: 10.1016/j.jece.2013.02.002.

Stefaniuk, M., Oleszczuk, P. & Ok, Y. S. 2016 Review on nano zerovalent iron (nZVI): from synthesis to environmental applications. *Chemical Engineering Journal* **287**, 618–632.

Stern, B. R. & Lagos, G. 2008 Are there health risks from the migration of chemical substances from plastic pipes into drinking water? A review. *Human and Ecological Risk Assessment* **14** (4), 753–779.

Water Environment Federation & American Public Health Association 2005 *Standard Methods for the Examination of Water and Wastewater*. American Public Health Association (APHA), Washington, DC, USA.

Xi, Y., Mallavarapu, M. & Naidu, R. 2010 Reduction and adsorption of Pb^{2+} in aqueous solution by nano-zero-valent iron – a SEM, TEM and XPS study. *Materials Research Bulletin* **45** (10), 1361–1367.

Zhang, Y., Oldenburg, C. M. & Benson, S. M. 2004 Vadose zone remediation of carbon dioxide leakage from geologic carbon dioxide sequestration sites. *Vadose Zone Journal* **3** (3), 858–866.

Zhao, Z., Liu, J., Tai, C., Zhou, Q., Hu, J. & Jiang, G. 2008 Rapid decolorization of water soluble azo-dyes by nanosized zero-valent iron immobilized on the exchange resin. *Science in China Series B: Chemistry* **51** (2), 186–192.

First received 4 May 2017; accepted in revised form 1 November 2017. Available online 21 November 2017